Magnetostratigraphy and Chronology of the Lower Pleistocene Primate Bearing Dafnero Fossil Site, N. Greece

Mouloud Benammi, Elina Aidona, Gildas Merceron, George Koufos, Dimitris Kostopoulos

quaternary

MDPI

Article

Magnetostratigraphy and Chronology of the Lower Pleistocene Primate Bearing Dafnero Fossil Site, N. Greece

Mouloud Benammi [1], Elina Aidona [2], Gildas Merceron [1], George D. Koufos [3] and Dimitris S. Kostopoulos [3,*]

1 Laboratoire Paléontologie, Evolution, Paléoécosystèmes, Paléoprimatologie (PALEVOPRIM) UMR 7262 CNRS INEE, Université de Poitiers UFR SFA, F-86022 Poitiers, France; mouloud.benammi@univ-poitiers.fr (M.B.); gildas.merceron@univ-poitiers.fr (G.M.)
2 Department of Geophysics, School of Geology, Aristotle University of Thessaloniki, GR-54124 Thessaloniki, Greece; aidona@geo.auth.gr
3 Laboratory of Geology & Palaeontology, School of Geology, Aristotle University of Thessaloniki, GR-54124 Thessaloniki, Greece; koufos@geo.auth.gr
* Correspondence: dkostop@geo.auth.gr; Tel.: +30-231-099-8540

Received: 10 June 2020; Accepted: 23 July 2020; Published: 26 July 2020

Abstract: This paper aims to contribute to the stratigraphic and geochronological evaluation of the primate bearing Dafnero fossil site of Northern Greece by means of lithostratigraphic, paleomagnetic and paleontological analyses. The 60 m thick fossiliferous deposits of fluviatile origin are recognized as representing a typical braided-river sequence unconformably overlying molassic sediments. Rock magnetic investigations indicate the presence of both medium and low coercivity minerals. Paleomagnetic sampling of the Dafnero sediments yielded a stable magnetic remanence, and the characteristic remanent magnetization directions pass reversal test with dual polarity. Based on calibration from mammal fossils, the normal polarity magnetozone N1 located in the upper third of the studied section could correlate with chron C2n (the Olduvai subchron), suggesting that the fossil horizon is within C2r with an extrapolated age of 2.4–2.3 Ma and rather closer to the upper age limit. The results allow the re-calibration of several middle Villafranchian assemblages of S. Balkans and the correlation of the corresponding mammal fauna with the environmental shifts of Praetiglian, as it is recorded in climatostratigraphic data from the Black Sea.

Keywords: magnetostratigraphy; biochronology; lower Pleistocene; Villafranchian; Balkans

1. Introduction

Magnetostratigraphy has proven to be a very useful tool for dating and correlation purposes in different geological ages and depositional settings. Magnetostratigraphic studies are deeply involved in the dating of Pliocene to Pleistocene mammal sites in the Mediterranean region and often significantly contribute to the discussion of the *Homo* dispersal in Europe (e.g., [1–11]). Although not so common, several magnetostratigraphic studies have been conducted during the last few decades in Greece to contribute to the investigation of various geo-issues [12–17] (among others). However, the ones corresponding to Neogene and Quaternary fossil mammal localities are very limited despite the numerous fossiliferous sites [18–23].

The fossiliferous locality of Dafnero in Western Macedonia, Greece, was discovered in early 1990s [24]. Systematic excavations until 1994 yielded an important though relatively poor Early Pleistocene mammal assemblage [25–28]. From 2010 onwards, new field campaigns conducted by a Franco-Hellenic team (Laboratory of Geology and Paleontology of the Aristotle University

of Thessaloniki, AUTh, Greece, and the Laboratoire Paléontologie Evolution Paleoecosystémes Paléoprimatologie PALEVOPRIM, CNRS-INEE and Université de Poitiers, France) on the original (Dafnero-1, DFN) and two new sites (Dafnero-2, DFN2; Dafnero-3, DFN3) significantly enriched the Dafnero fossil sample (more than 1000 identifiable specimens so far) and faunal list [29,30].

Dafnero mammal fauna is central to a group of Southern Balkan local faunas representing the Early Pleistocene (middle-late Villafranchian) in SE Europe and reveals strong resemblance with a set of Western European local mammal assemblages (e.g., Villaroya, La Puebla de Valverde, Spain; St. Vallier, Chilhac, Senèze, France; Coste St. Giacomo, Italy) spanning from 2.5 to 2.0 Ma (e.g., [31]). In the absence, however, of independent and more detailed dating, the available biochronological data of S. Balkans do not allow conclusions to be drawn regarding the spatio-temporal differentiation between the middle Villafranchian mammal faunas of Western and Eastern Europe or diachronicity phenomena to be traced. Furthermore, recent reviews of the dating of various important sites in Western Europe (e.g., [11,32–34]) have partially altered our perceptions of the faunal succession during the Early Pleistocene period. Besides, DFN3 is one of the relatively few Eurasian sites bearing remains of *Paradolichopithecus*, a terrestrial papionin monkey of questionable phylogenetic relationships [29], and, therefore, the chronology of the site is essential to the discussion of the evolution of this lineage.

The aim of the present study is to provide a better age estimation of the local fauna of Dafnero by means of combined paleomagnetic data and biochronological evidence in order to contribute to a finer resolution of the succession of mammal faunas in the Balkan Peninsula during the Early Pleistocene period and its causation and to allow for better future comparisons of the relationships with corresponding faunas of Western Europe.

2. Geographical and Geological Settings

The fossiliferous locality of Dafnero (DFN) is located at the SW slopes of Vourinos Mt, at about 30 km southwest of Kozani city, NW Greece (40°10′16″ N, 21°33′35″ E) and near the homonymous village (Figure 1A). The Quaternary physiogeography of the studied area is dominated by the complex ravine system associating the Haliakmon River valley that extends in a northwesterly direction from close the Greco-Albanian borders to the Sarantaporos Mountain [29]. Geotectonically, it is placed along the eastern margins of the Mesohellenic Basin (MHB), an Oligo-Miocene post-orogenic trough with a long detrital sedimentary infill (see [35–37]).

In the particular area around Dafnero, the Triassic-Jurassic limestones and Jurassic ophiolites of the basement are unconformably underlying by turbidite to fan-deltas alternations ascribed to the Miocene Tsotilion (or Tsotili) Formation (Fm) of MHB ([36], and references therein). Tsotylion Fm appears in the lower part of the studied section as a ~30 m thick lithostratigraphic unit (LU) of gray-green conglomerates with siltstone and sandstone intercalations (LU0 in Figure 1B). A ~60 m thick unit of likely fluvio-terrestrial origin unconformably overlies Tsotylion deposits, though their contact is hidden mainly due to extensive erosion and vegetation. This upper fossiliferous part of the stratigraphic section is subdivided into three subunits from the base to the top: a ~15 m thick coarse conglomerate (LU1 in Figure 1B), followed by 12–14 m thick yellowish to orange colored silty sands intercalated with grey to whitish dense and thick conglomerates (LU2 in Figure 1B) and finally by ~30 m thick alternations of reddish silty sands, and gravels with paleosoil intercalations (LU3 in Figure 1B). The LU1 subunit represents the proximal (L-bar dominant), LU2 the ideal (L-bars and T-bars), and LU3 the distal (T-bar dominant) parts of a rather typical braided-river sequence. The fossiliferous sites of Dafnero (DFN, DFN2, and DFN3) are placed at the base of LU2. DFN-DFN3 level is 2 m above the top of LU1 and half meter below a 1–2 m thick conglomerate (Figure 1C). DFN and DFN2 are single spots exhaustively excavated, whereas DFN3 appears with eight successive spots [29], extremely dense in fossils (Figure 1C) that, however, usually suffer from fracturing and diagenetic softening.

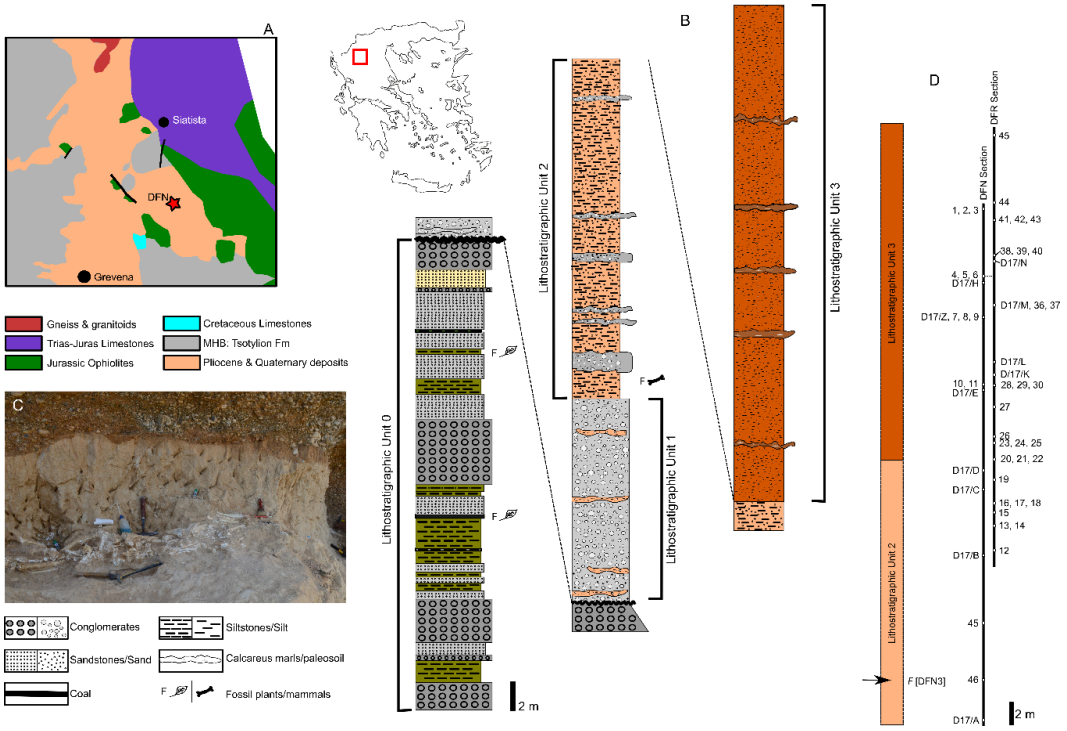

Figure 1. Geographic and geological setting of the Dafnero fossil sites. (**A**) Simplified geological map of the studied area (from [37], redesigned). (**B**) Composite stratigraphic section of Dafnero sedimentological sequence; F denote fossiliferous level. (**C**) Example of fossil accumulation at DFN3 fossil site indicating local sedimentological setting. (**D**) Position of palaeomagnetic sampling and correlation between the two sampled sections from Dafnero area.

3. Paleomagnetic Sampling and Laboratory Procedures

The topography at the Dafnero site exploited for fossils is very rough, with very steep slopes. Paleomagnetic samples were taken along two largely overlapping and lithostratigraphically correlated sections (DFN and DFR), covering the uppermost and fossiliferous part of the local stratigraphy (i.e., the entire LU2 and the greatest part of LU3 subunits; Figure 1D). The first section was located along the ravine leading to the fossiliferous site DFN3, while the second one a few tens of meters to the east. Due to the inconvenient nature of the deposits for magnetostratigraphic purposes (conglomerate intercalations, gravel lenses etc.), a total of 30 unevenly spaced stratigraphic levels have been sampled by oriented hand samples and drilling cores: twelve levels are from the 44.5 m thick DFN section and 18 from the 37 m thick DFR section (Figure 1D). Eleven of the sampled levels belong to LU2 and the rest to LU3.

Paleomagnetic measurements were conducted using a JR6 magnetometer housed in a magnetically shielded room at the PALEVOPRIM, University of Poitiers. After the measurement of the natural remanent magnetization (NRM), samples were submitted to stepwise demagnetization both thermal (TH) and alternating field (AF), with steps of 5 to 10 mT, up to maximum field of 40 or 70 mT. In order to better constrain the magnetic mineralogy, a set of rock magnetic experiments were conducted both in PALEVOPRIM and in the Palaeomagnetic Laboratory of AUTh. The acquisition of isothermal remanent magnetization (IRM) was performed, following by the stepwise thermal demagnetization of three-axis differential IRM. Magnetic fields of 1, 0.4 and 0.12 T were successively applied to z, y and x axes, respectively, before their thermal demagnetization [38].

The specimens were subjected to stepwise thermal demagnetization up to 600 °C, using a magnetic measurement thermal demagnetizer shielded furnace (MMTD80). Additionally, thermomagnetic analyses on the Curie balance were carried out on selected samples in open air.

In order to determine polarities and directions of the NRM, demagnetization results were plotted on orthogonal vector diagrams [39] and on stereographic projections. The directions of the Characteristic Remanent Magnetization (ChRM) were isolated by a principal component analysis [40] and mean directions were determined by Fisher statistics [41].

Most of the studied samples show two components of magnetization. Sometimes the demagnetization occurs along a large circle, confirming the existence of two magnetic components whose blocking-field spectra are superimposed. The thermal demagnetization proved to be effective and standard thermal demagnetization techniques were applied to groups of samples in order to compare the direction with the ones obtained using the alternating field demagnetization.

4. Paleomagnetic Results

4.1. Magnetic Mineralogy

For the acquisition of the IRM, the samples were saturated in successive steps using an electromagnet. In all cases, the acquisition curves rise steeply in low field and reach more than 90% of saturation remanence at 200 mT, indicating the presence of low coercivity minerals. After that point, there is a gradual increase of IRM that generally reaches saturation beyond 0.4 or 0.5 T (Figure 2A).

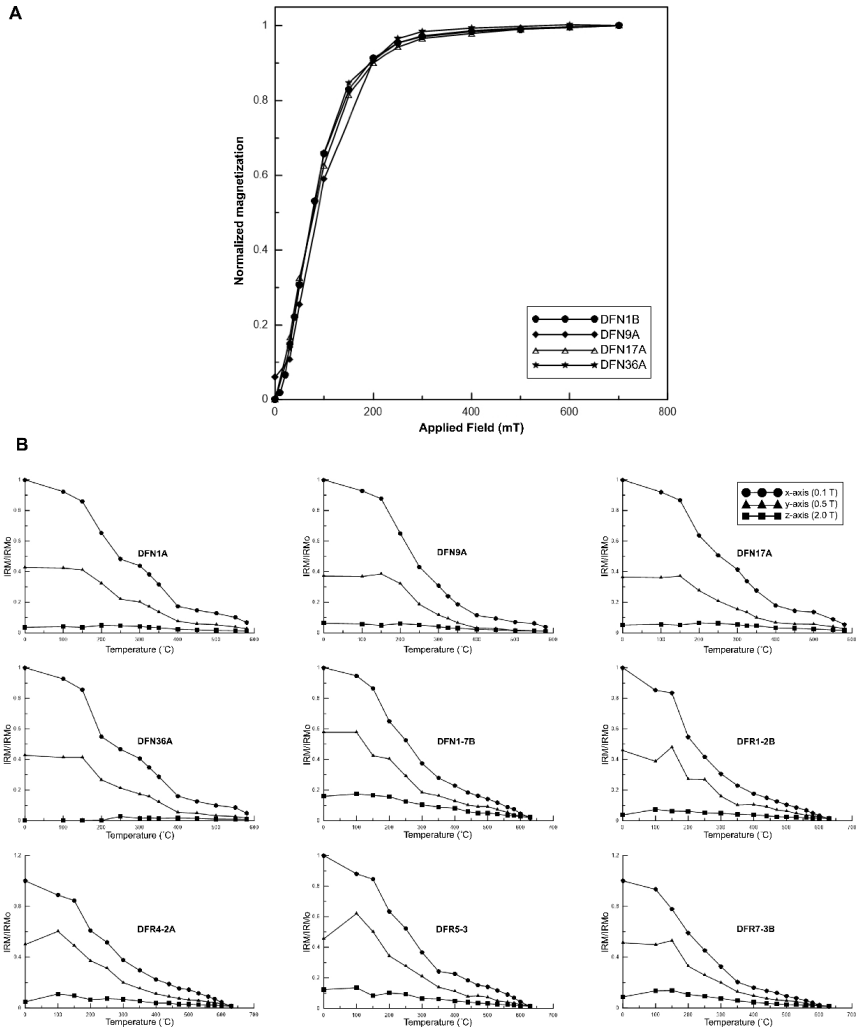

Figure 2. (**A**) Stepwise acquisition of an isothermal remanent magnetization (IRM) up to fields of 700 mT. (**B**) Examples of thermal demagnetization of a composite IRM acquired on three orthogonal axes.

The results of the thermal demagnetization of the three axis IRM are given in Figure 2B, where the individual components of the IRM along the x, y, and z axes are shown. A similar trend is observed in all samples; the soft (0.12 T) component is pronounced and demonstrates the prominent inflexion around 400 °C, suggesting the presence of Ti-poor titanomagnetite. This component diminishes up to a maximum unblocking temperature of approximately 580 °C, indicating magnetite as the main magnetic mineral (Figure 2B). The results of the combination of IRM acquisition and thermal demagnetization analysis indicate that both low coercivity minerals as titanomagnetite and magnetite are the main carriers of magnetization in the studied sediments.

4.2. Curie Balance

The results of the Curie balance analysis are shown in Figure 3. In all cases the curves are not reversible, and two distinct Curie temperatures are present, one between 350 and 400 °C and a second one between 550 and 580 °C. The presence of two different picks of Curie temperature corresponds to the presence of the titanomagnetite and magnetite-type magnetic minerals. In the case of the sample DFR7 the cooling curve is higher than the heating curve, indicating the formation of new ferromagnetic minerals during heating.

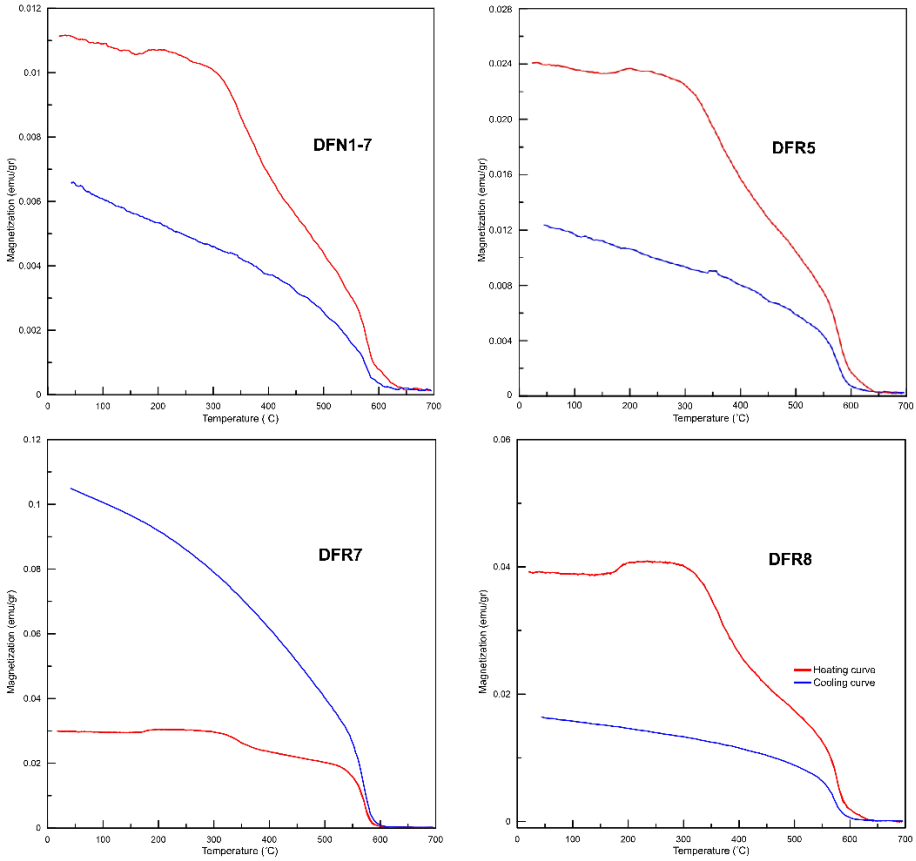

Figure 3. Variation of magnetization with temperature showing the magnetic behavior of representative samples.

4.3. Natural Remanent Magnetization

All samples were submitted to stepwise demagnetization either by heating (9–12 steps) or by alternating field up to 70 mT. The majority of the samples (86%) are of good quality as is shown in the representative demagnetization diagrams (Figure 4). Both TH and AF demagnetization procedures give interpretable results. The specimens showed a stable behavior during demagnetization (Figure 4). Furthermore, during the demagnetization at least two distinct magnetic components have been revealed.

A secondary component is parallel to the present field in geographic coordinates and was isolated at low temperatures (110–200 °C/10 mT; Figure 4A,B,E,F). This component represents most probably a viscous overprint acquired during the past 0.78 Ma. A second component was visible between temperatures ranging from 200 °C to 500–550 °C (Figure 4B), or 10 to 70 mT and its direction is well determined (Figure 4A,C–F).

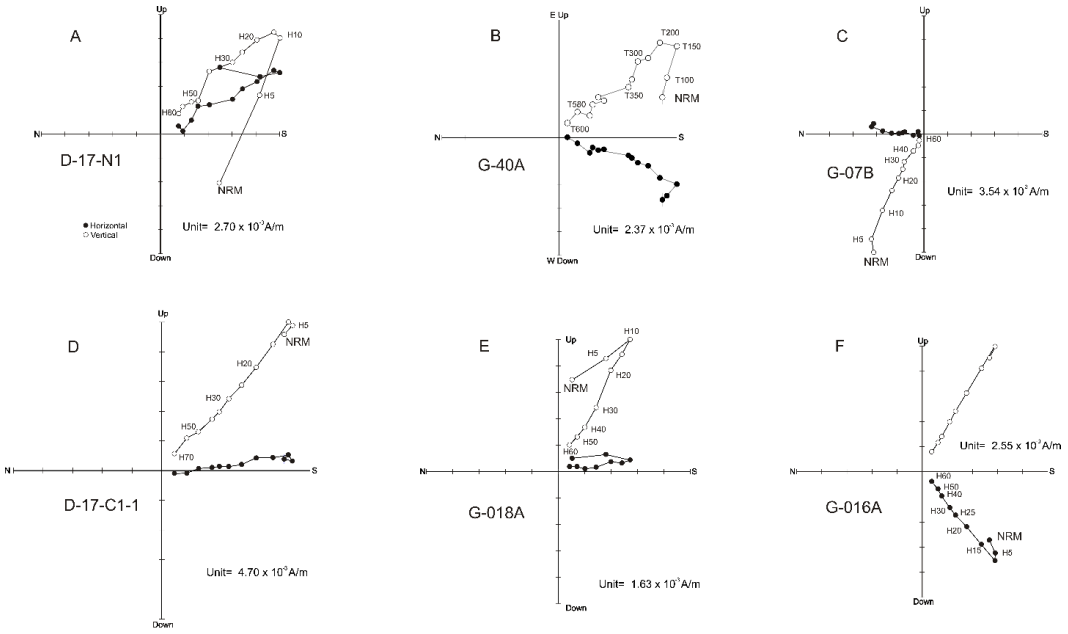

Figure 4. Orthogonal vector plots of alternating field (AF) and thermal (TH) demagnetization of representative samples (**A**–**F**) of Dafnero sections. Solid circles indicate horizontal component; open circles indicate vertical component. Demagnetization steps in mT or °C. NRM is the natural remanent magnetization.

We obtained reliable characteristic remanent magnetization (ChRM) directions from Dafnero sections. Specimens showing incoherent directions during the stepwise demagnetization were not used for the final calculation of the mean direction. The directions of the high stability component were calculated by principal component analysis [40]. The paleomagnetic directions characterized by northerly declination and positive inclination or southerly declination and negative inclination were interpreted as of normal or reversed polarity, respectively. The polarities of the high stability component were found to be normal or reversed, suggesting that the remanent magnetization is primary and can be referred to as the characteristic component of NRM (ChRM). The Fisher statistics [41] were applied, in order to calculate the mean directions for both sections, and plotted on stereographic diagrams (Figure 5). The mean direction of the normal polarities is declination = 359.9°, inclination = 50.9°, (α95= 12.8°, K=6.31) and for the reverse polarities, declination = 177.4°, inclination = −56.4° (α95 = 5.6°, K = 13.8). To evaluate the reliability of our results, they were submitted to the reversal test [42]. For our section, the angle calculated between mean directions of the normal and reversed polarity is 5.7°. Mean directions are not exactly antipodal, and hence, passed the test with B classification [42].

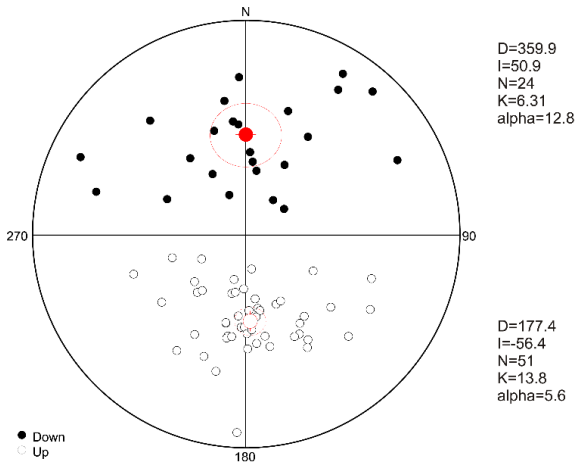

Figure 5. Stereographic projection of characteristic directions (normal and reversed polarities) isolated from the studied samples. Red dot is the calculated mean direction, while the red circle around it represents the 95% confidence limit [41]. D, I and alpha in degrees (°).

4.4. Magnetostratigraphic Interpetation

The presence of normal and reverse polarities suggests that the NRM of the samples can be considered as primary. To evaluate the origin and nature of the paleomagnetic record, for magnetic polarity stratigraphy, the characteristic magnetizations were examined. Some samples were excluded because of inconsistency of directions during the demagnetization process, or due to their weak magnetization. A magnetic polarity sequence is presented using the virtual geomagnetic pole (VGP) latitude of the characteristic paleomagnetic directions (Figure 6). In the lower part of the section, results are of reversal polarity. This polarity interval (R1) is represented by 16 successive levels (from both the DFN and DFR sections; Figure 6). Above it, an interval of 9.5 m thick in the DFN section (three levels) and of 5 m thick in the DFR section (two levels) shows normal polarity (N1). The top reversed polarity interval (R2) is represented by one site at the DFN section and three at the DFR.

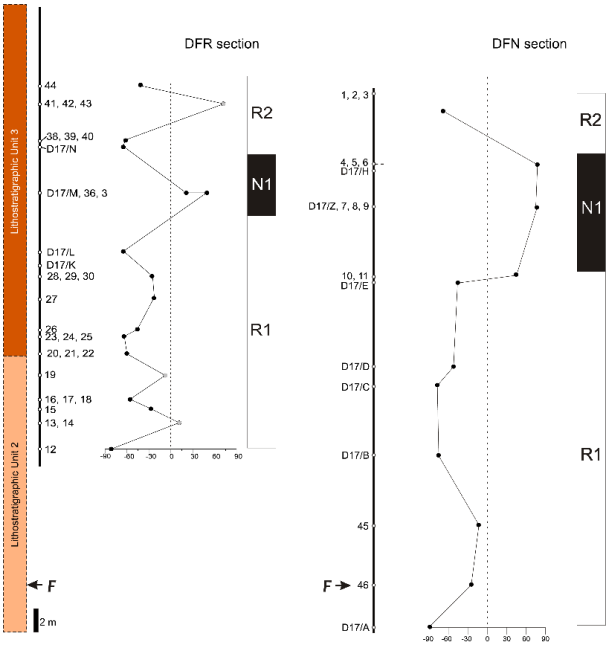

Figure 6. Magnetostratigraphy of the Dafnero sections. Normal and reversed polarities are represented by positive and negative VGP latitudes, respectively. Black dots represent reliable directions used for the magnetostratigraphy while grey dots mark discarded unsuitable samples.

5. Age Estimation

The present magnetostratigraphic study meets most of the proposed quality criteria [43] in order to provide reliable time calibration. Hence, results are from a well-studied and tectono-stratigraphically controlled basin (e.g., [36]), and they are based on two lateral profiles unambiguously correlated by lithostratigraphic criteria allowing both reproducibility of magnetic data and reduction of sampling failures. The two studied sections are rather short, but both reach the maximum possible for this particular area and local depositional settings. Laboratory treatment comprises all necessary procedures (i.e., stepwise demagnetization to identify different magnetic components, investigation of magnetic carriers, Curie balance tests), whereas ChRM directions are fitted using principal component analysis (PCA). Although magnetotratigraphic data must be kept as independent as possible from biochronological ones (e.g., [43]), local biochronological evidence is necessary in order to constrain possible correlation(s) with Geomagnetic Polarity Time Scale (GPTS).

5.1. Biochronological Frame

The continental deposition in the studied area seems to have started no earlier than 3.5 Ma according to micropaleontological data from neighboring lithostratigraphic sections along the Pramoritsas River [44,45]. Indeed, the oldest known land-fauna comes from the nearby Milia fossil site, indirectly dated to about 3.5–3.0 Ma [46,47]. The mammal assemblage of Milia including taxa such as *Mammut borsoni*, *Anancus arvernensis*, *Agriotherium*, *Tapirus arvernensis*, *Hipparion*, *Stephanorhinus jeanvireti*, *Hystrix refossa*, *Sus arvernensis* and *Alephis* implies an early Villafrachian spectrum, certainly more primitive than that of Dafnero. The list of mammals recognized so far from the Dafnero fossil site (incorporating DFN, DFN2 and DFN3 evidence) includes at least 19 taxa (Table 1) ranging in size from that of a hedgehog to a rhino.

Table 1. Faunal association of Dafnero, Greece, combining evidence from DFN, DFN2 and DFN3 sites. Data from [24–30,48], and pers. data.

Primates	Perissodactyla
Paradolichopithecus aff. *arvernensis*	*Stephanorhinus* ex gr. *etruscus*
Carnivora	*Equus stenonis* (*'vireti'* morphotype)
Ursus etruscus	**Giraffidae**
Nyctereutes megamastoides	*Palaeotragus inexspectatus*
Vulpes alopecoides	**Cervidae**
Baranogale aff. *helbingi*	*Metacervocerus rhenanus*
Chasmaporthetes lunensis	*Eucladoceros ctenoides*
Homotherium latidens	**Bovidae**
Lynx issiodorensis	*Gallogoral meneghinii*
Rodentia	*Gazellospira torticornis*
Castor sp.	*Gazella bouvrainae*
Insectivora	*Capra*? sp.
Erinaceus sp.	

Taxa in red represent new entries compared to [48].

The association of Dafnero mammals is unambiguously representing a typically Villafranchian assemblage [31]. The combination of *Paradolichopithecus arvernensis*, *Ursus etruscus*, *Vulpes alopecoides*, *Lynx issiodorensis*, *Homotherium latidens*, *Stephanorhinus* ex. gr. *etruscus* and *Gazellospira torticornis*, roughly frame the Dafnero fauna between 3.0 and 1.6 Ma (Figure 7B). The strong signal of *Nyctereutes megamastoides* and the absence of the *Canis etruscus-Canis arnensis* group are rather suggestive of a pre-Olduvai age [49] that is also consistent with the presence of *Chasmaporthetes lunensis* and *Gazella* [31,50,51]. On the other hand, the co-occurrence of *Palaeotragus inexspectatus*, *Metacervoverus rhenanus*, *Eucladoceros ctenoides* and *Gallogoral meneghinii* indicate an age younger than the Pliocene-Pleistocene boundary (~2.6 Ma) [31,50] (Figure 7B). Finally, the strong resemblance of the stenonoid horse from Dafnero with the *Equus stenonis* "*vireti-pueblensis*" morphotype [26] further

restricts the fauna between 2.5 and 2.0 Ma. As a whole, the Dafnero mammal fauna shows the greatest faunal similarity at the species level with faunas like those from Saint-Vallier (France), La Puebla de Valverde (Spain) and Coste St Giacomo (Italy) to cite the most important ones, all placed within the 2.5–2.0 Ma time-interval [32,34,50,51].

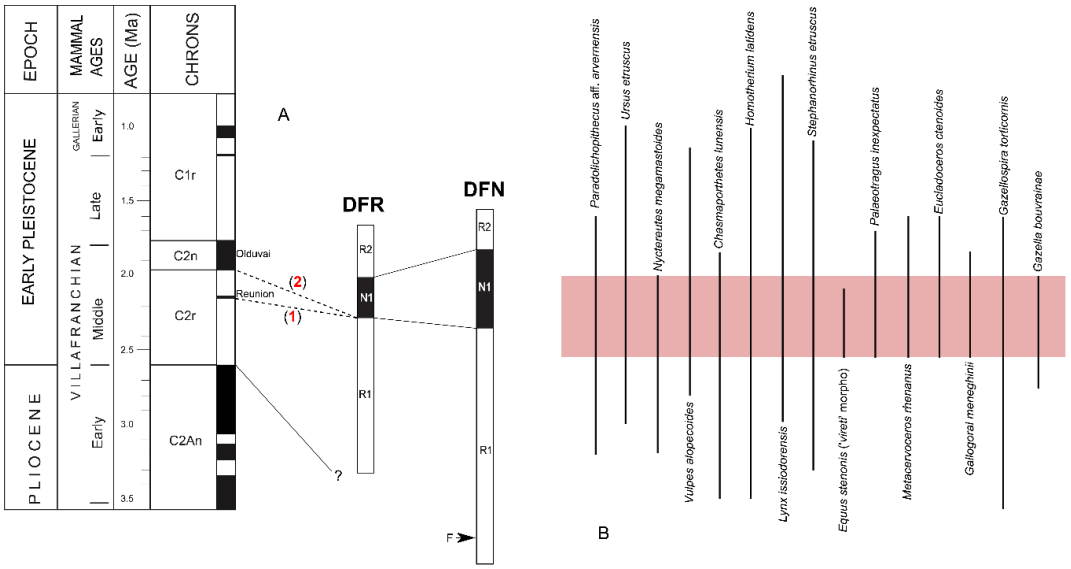

Figure 7. Chronology of Dafnero fossil sites. (**A**) Magnetostratigraphic correlation among the Dafnero sections, and GPTS [52]; two alternative scenarios are given (1): correlation of N1 zone with the Réunion subchron, and (2): correlation of N1 zone with the Olduvai subchron (for discussion see text). (**B**) Biochronological frame (reddish bar) provided by Dafnero mammal association; vertical lines represent the known time-range of 15 out of 19 mammal taxa recorded at Dafnero.

5.2. Correlation with GPTS

Our paleomagnetic data would allow for refining the chronology of Dafnero and placing it into a broader timeframe, if these could successfully be correlated with GPTS on the Matuyama Chron as indicated by biochronological evidence. During this period several magnetic polarity reversals are recorded, with the three main reverse Chrons C2r.2r (2.58 Ma to 2.15 Ma), C2r.1r (2.13 Ma to 1.94 Ma), and C1r.2r (1.78 to 1.07Ma) delineating the short normal Réunion subchron, C2r.1n (2.15–2.13 Ma), and the normal Olduvai subchron, C2n (1.94 to 1.78 Ma) [52]. A correlation with the uppermost part of the Matuyama Chron (1.07 to 0.781 Ma) is obviously too young, leading to unrealistic chronologies for the Dafnero fauna.

The magnetostragigraphic study of Dafnero sediments revealed the presence of a long zone of reverse polarity, interrupted by a short normal polarity zone (N1), maximally reaching 10 m of thickness. The Dafnero fossil site is placed within the lower reversed polarity magnetozone R1, 26.5 m below the R1/N1 boundary. The available data cannot unequivocally distinguish between a possible correlation of the normal polarity zone N1 recorded at Dafnero with either C2n (i.e., the Olduvai subchron) or the shorter C2r.1n (i.e., the Réunion subchron) (Figure 7A). Therefore, we explore which of the two scenarios (i.e., either N1- Réunion or N1-Olduvai correlation) is the most likely.

Olduvai spans a period of 167 kyrs (1.945–1.778 Ma) while Réunion shows a much shorter time interval of 20 kyrs (2.148–2.128 Ma). Taking into account the above time spans and assuming an even and stable sedimentation rate for the Dafnero section, a correlation of the 9.5 m thick N1 zone with the Olduvai subchron would allow estimating a mean accumulation rate of about 5.68 cm/kyr for the stratigraphic unit represented by this normal zone (N1) (option (2) in Figure 7A). Similarly, a mean accumulation rate of 47.5 cm/kyr is estimated in the case of a N1—Réunion correlation (option (1) in Figure 7A). Extrapolating assumptions and results to the whole Dafnero section, the fossil layer DFN3

would be dated 466.5 kyrs below the Olduvai or 55.8 kyrs below the Réunion subchron. Hence, Dafnero fossil fauna would be suggested as 2.4 Ma ("Olduvai" scenario) or 2.2 Ma ("Réunion" scenario) old.

Both alternative estimated ages for the Dafnero fauna do not contradict local biochronogical evidence. Assessed mean accumulation rates are also within the broader ranges proposed for fluviatile deposits in both scenarios [53–55]. Nevertheless, empirical data from deposits of similar lithology across Eurasia suggest that Réunion subchron rarely overpasses 5 m (usually around 2.5 m) in thickness in the local stratigraphic records, whereas Olduvai subchron is usually registered by a thickness of about 10 m or more [5,7,11,32,56]. This would mean that it may be hard to trace Réunion in continental sequences due to its short duration, especially in cases such as the lower part of the Dafnero section, where distance between sampling horizons sometimes reaches 4 m. Keeping all these in mind, we suggest that N1 normal zone of Dafnero magnetostratigraphic section would make a correlation with C2n, i.e., with the Olduvai subchron, more likely. This would allow us to estimate the age of the Dafnero fauna between 2.4 and 2.3 Ma, and rather closer to 2.3 Ma, adopting a more relaxing accumulation rate estimation of 5–7 cm/kyrs for the complete section.

6. The Southern Balkan Middle Villafranchian Faunal Succession

Among the Greek Pliocene to Pleistocene faunas ([48], and references therein), the Dafnero mammal assemblage shows the highest similarity at the species level with those from Sesklo (upper horizon; Dice similarity index, DSI: 80%), Vatera (DSI: 56%), and Volakas (DSI: 71%), all of them characterized by the association of *Nyctereutes megamastoides*, *Stephanorhinus* ex. gr. *etruscus*, *Equus stenonis* ("*vireti-pueblensis*" morphotype), *Palaeotragus inexspectatus*, *Metacervocerus rhenanus* and *Gazellopsira torticornis*, and the common presence of *Eucladoceros ctenoides*, *Gallogoral meneghinii* and *Gazella bouvrainae* (Table 2). The high homogeneity shown by these local assemblages also suggests a rather temporal proximity, and based on the new age estimation of the Dafnero fauna, they can all be likely dated to around 2.3 Ma and safely within the 2.4–2.2 Ma time-frame. The proposed dating is also consistent with the absence of *Pachycrocuta brevirostris*, and *Canis* ex gr. *etruscus* from them, as both taxa are known to appear in Europe after 2.1–2.0 Ma [49,57].

The rich Bulgarian fauna of Varshets shares several taxa in common with the Dafnero-Sesklo-Vatera-Volakas palaeocommunity. Nevertheless, the presence of *Nyctereutes* cf. *tingi*, the more primitive features of *Gazellospira* sp. and the evolutionary stage of *Martes* and *Ursus* indicate an older age, likely older than St. Vallier [58,59] but still younger than Roccaneyra. Following the proposed ages by Nomade et al. [34] for these two French sites (2.5 Ma and 2.6 Ma, respectively) and the new dating for Dafnero, the Varshets fauna would be preferably placed at the beginning of middle Villafranchian, within the 2.4–2.5 Ma interval. Partially differentiated from the scheme proposed by Spassov [59], we think that Varshets represents the beginning of MN17 in S. Balkans (though we still miss large mammal faunas equivalent to the Montopoli Faunal Unit), whereas Dafnero represents the top of MN17a (MN17a, sensu [34]). It is, however, obvious that MN and MNQ subdivisions do not fully coincide across northern Mediterranean. A new comparative study is, therefore, needed, especially in the light of current magnetostratigraphic and/or absolute datings that seem to mismatch or even contradict biochronological evidence (e.g., La Puebla de Valverde fauna compared to those of St. Vallier, Senèze, and Coste St. Giacomo or Villaroya fauna compared to those of Dafnero, Chilhac and St. Vallier) [11,32,34,50,51].

The high incidence and geographical extent of the Varshets-Dafnero type fauna from the S. Balkans to the Minor Asia coasts likely suggests the predominance of a particular ecoregion. Several regional environmental changes occur within the 2.5–1.8 Ma time interval noticed in the pollen diagram of the DSDP site 380 in Black Sea, the closest one to the Dafnero site [60]. According to Popescu et al. [60], the Pollen zone three (624–603 m) that corresponds to the 2.6–2.4 Ma interval, representing the regional Praetiglian, is characterized by low percentages of mesothermic and high of steppe (>25%) elements, altogether suggesting very open vegetation and expansion of the Anatolian *Artemisia* steppe due to the establishment of cooler and drier climatic conditions. Such a shift to more open and dry habitats is

well supported by available dental microwear data on ruminants from both Sesklo and Dafnero, as well as on post-cranial ecometrics of *G. torticornis* from the Dafnero site [61–63].

Table 2. Taxonomic comparison among several middle Villafranchian Greek large mammal faunas. Data from [48,64,65], and pers. data.

Main Large Mammal Taxa	DFN	SES	VTR	VOL
Paradolichopithecus arvernensis	aff			
Anancus arvernensis				
Mammuthus meridionalis			cf.	
Nyctereutes megamastoides				
Vulpes alopecoides/praecorsac		cf.		
Ursus etruscus		cf.		
Baranogale helbingi	cf.			
Chasmaporthetes lunensis				
Pliocrocuta perrieri				?
Homotherium latidens			sp.	
Megantereon megantereon				
Lynx issiodorensis				
Meles thorali				
Stephanorhinus ex gr. *etruscus*		sp.	cf.	indet.
Equus stenonis 'vireti group'				
Palaeotragus inexspectatus			cf.	
Eucladoceros ctenoides				
Metacervocerus rhenanus		aff.	cf.	
Croizetoceros ramosus				
Leptobos sp.				
Gallogoral meneghinii				
Gazellospira torticornis			cf.	cf.
Gazella borbonica			aff.	
Gazella bouvrainae			cf.	
Gazella aegea				
Euthyceros thessalicus				
Procamptoceras			?	

DFN: Dafnero; SES: Sesklo; VTR: Vatera; VOL: Volakas. Certain species occurrences are marked as black cells; grey cells indicate taxa most likely (*confer*; cf.) or conditionally (*affinis*; aff.) identified at the species level; white cells indicate problematic or insufficiently known taxa.

7. Conclusions

The paleomagnetic and rock magnetic results of the Dafnero site indicate that the dominant detrital magnetic minerals are titanomagnetite and magnetite. The characteristic remanent magnetization is of primary origin based on the positive reversal test. Magnetostratigraphic analysis supported by biochrononologic evidence demonstrates that the normal polarity zone detected at Dafnero section could be better correlated with chron C2n, suggesting that the fossil site is placed within C2r and deliver an estimated age for the Dafnero fauna at 2.3 Ma. The results allow us to provide a revised age calibration of several key large mammal assemblages of the middle Villafranchian of S. Balkans and to correlate them with climatostratigraphic data from the Black Sea.

Author Contributions: Conceptualization, G.M. and D.S.K.; Data curation, M.B., E.A. and D.S.K.; Formal analysis, M.B., E.A. and D.S.K.; Funding acquisition, G.M. and D.S.K.; Methodology, M.B., E.A. and D.S.K.; Project administration, G.M. and D.S.K.; Software, M.B. and E.A.; Supervision, D.S.K.; Validation, M.B., E.A., G.D.K., G.M. and D.S.K.; Visualization, D.S.K.; Writing—original draft, M.B., E.A., G.D.K., G.M. and D.S.K.; Writing—review and editing, E.A. and D.S.K. All authors have read and agreed to the published version of the manuscript.

Funding: Excavations at Dafnero were supported by the CNRS, France, grant number PICS5185; 2010–2013 and IEA 08245 (2019-2021), and the National Geographic Society, grant 9903-16; 2016–2017.

Acknowledgments: We would like to thank Frank Guy, Xavier Valentin, Emilie Berlioz, and especially Anastasia Gkeme and Chris-Alexander Plastiras for their help on the field. We express our gratitude to G. Muttoni for his suggestions and comments on the correlation results.

Conflicts of Interest: The authors declare no conflict of interest.

References

1. Torre, D.; Albianelli, A.; Bertini, A.; Ficcarelli, G.; Masini, F.; Napoleone, G. Paleomagnetic calibration of Plio-Pleistocene mammal localities in central Italy. *Acta Zool. Cracov.* **1996**, *39*, 559–570.
2. Albianelli, A.; Azzaroli, A.; Beriini, A.; Ficcarelli, G.; Napoleone, G.; Torre, D. Paleomagnetic and palynologic investigations in the upper Valdarno basin (central Italy): Calibration of an early Villafranchian fauna. *Riv. Ital. Paleontol. Stratigr.* **1997**, *103*, 111–118.
3. Sen, S. Magnetostratigraphic calibration of the Neogene mammal chronology. *Palaeogeogr. Palaeoclimatol. Palaeoecol.* **1997**, *133*, 181–204. [CrossRef]
4. Sen, S. Magnetostratigraphy of the Villafranchian mammal locality of Saint-Vallier (Drome). *Geobios* **2004**, *37*, 58–61. [CrossRef]
5. Oms, O.; Dinares-Turell, J.; Agustı, J.; Pares, J. Refinements of the European Mammal Biochronology from the Magnetic Polarity Record of the Plio–Pleistocene Zujar section, Guadix-Baza Basin, SE Spain. *Quat. Res.* **1999**, *51*, 94–103. [CrossRef]
6. Agusti, J.; Cabrera, L.; Garces, M.; Krijgsman, W.; Oms, O.; Pares, J.M. A calibrated mammal scale for the Neogene of Western Europe: State of the art. *Earth Sci. Rev.* **2001**, *52*, 247–260. [CrossRef]
7. Scott, G.R.; Gibert, L.I.; Gibert, J. Magnetostratigraphy of the Orce region (Baza Basin), SE Spain: New chronologies for Early Pleistocene faunas and hominid occupation sites. *Quat. Sci. Rev.* **2007**, *26*, 415–435. [CrossRef]
8. Madurell-Malapeira, J.; Minwer-Barakat, R.; Alba, D.M.; Garcés, M.; Gómez, M.; Aurell-Garrido, J.; Ros-Montoya, R.; Moyà-Solà, S.; Berástegui, X. The Vallparadís section (Terrassa, Iberian Peninsula) and the latest Villafranchian faunas of Europe. *Quat. Sci. Rev.* **2010**, *29*, 3972–3982. [CrossRef]
9. Muttoni, G.; Scardia, G.; Kent, D.V. Human migration into Europe during the late Early Pleistocene climate transition. *Palaeogeogr. Palaeoclimatol. Palaeoecol.* **2010**, *296*, 79–93. [CrossRef]
10. Muttoni, G.; Scardia, G.; Kent, D.V. Early hominins in Europe: The Galerian migration hypothesis. *Quat. Sci. Rev.* **2018**, *180*, 1–29. [CrossRef]
11. Pueyo, E.; Muñoz, A.; Laplana, C.; Parés, J. The Last Appearance Datum of *Hipparion* in Western Europe: Magnetostratigraphy along the Pliocene–Pleistocene boundary in the Villarroya Basin (Northern Spain). *Int. J. Earth Sci. (Geol. Rundsch)* **2016**, *105*, 2203–2220. [CrossRef]
12. Muttoni, G.; Kent, D.; Gaetani, M. Magnetostratigraphy of a Lower–Middle Triassic boundary section from Chios, Greece. *Phys. Earth Planet. Inter.* **1995**, *92*, 245–260. [CrossRef]
13. Muttoni, G.; Kent, D.; Brack, P.; Nicora, A.; Balini, M. Middle Triassic magnetostratigraphy and biostratigraphy biostratigraphy from the Dolomites and Greece. *Earth Planet. Sci. Lett.* **1997**, *146*, 107–120. [CrossRef]
14. Van Vugt, N.; Steenbrink, J.; Langereis, C.G.; Hilgen, F.J.; Meulenkamp, J.E. Magnetostratigraphy-based astronomical tuning of the early Pliocene lacustrine sediments of Ptolemais (NW Greece) and bed-to-bed correlation with the marine record. *Earth Planet. Sci. Lett.* **1998**, *164*, 535–551. [CrossRef]
15. Steenbrink, J.; Hilgen, F.J.; Krijgsman, W.; Wijbrans, J.R.; Meulenkamp, J.E. Late Miocene to Early Pliocene depositional history of the intramontane Florina–Ptolemais–Servia Basin, NW Greece: Interplay between orbital forcing and tectonics. *Palaeogeogr. Palaeoclimatol. Palaeoecol.* **2006**, *238*, 151–178. [CrossRef]
16. Cornée, J.-J.; Moissette, P.; Joannin, S.; Suc, J.-P.; Quillévéré, F.; Krijgsman, W.; Hilgen, F.; Koskeridou, F.; Münch, P.H.; Lécuyer, C.H.; et al. Tectonic and climatic controls on coastal sedimentation: The Late Pliocene–Middle Pleistocene of Northeastern Rhodes, Greece. *Sediment. Geol.* **2006**, *187*, 159–181. [CrossRef]
17. Snel, E.; Mărunţeanu, M.; Meulenkamp, J.E. Calcareous nannofossil biostratigraphy and magnetostratigraphy of the Upper Miocene and Lower Pliocene of the Northern Aegean (Orphanic Gulf–Strimon Basin areas), Greece. *Palaeogeogr. Palaeoclimatol. Palaeoecol.* **2006**, *238*, 125–150. [CrossRef]
18. Sen, S.; Valet, J.P. Magnetostratigraphy of late Miocene continental deposits in Samos, Greece. *Earth Planet. Sci. Lett.* **1986**, *80*, 167–174. [CrossRef]

19. Sen, S.; Koufos, G.; Kondopoulou, D.; Bonis, L. Magnetostratigraphy of the late Miocene continental deposits of the lower Axios valley, Macedonia, Greece. *Bull. Geol. Soc. Greece Spec. Issue* **2000**, *9*, 197–206.
20. Kostopoulos, D.S.; Sen, S.; Koufos, G.D. Magnetostratigraphy and revised chronology of the late Miocene mammal localities of Samos, Greece. *Int. J. Earth Sci.* **2003**, *92*, 779–794. [CrossRef]
21. Kondopoulou, D.; Sen, S.; Aidona, E.; van Hinsbergen, D.J.J.; Koufos, G. Rotation history of Chios Island, Greece since the Middle Miocene. *J. Geodyn.* **2011**, *51*, 327–338. [CrossRef]
22. Böhme, M.; Spassov, N.; Ebner, M.; Geraads, D.; Hristova, L.; Kirscher, U.; Kötter, S.; Linnemann, U.; Prieto, J.; Roussiakis, S.; et al. Messinian age and savannah environment of the possible hominin *Graecopithecus* from Europe. *PLoS ONE* **2017**, *12*, e0177347. [CrossRef]
23. Tourloukis, V.; Muttoni, G.; Karkanas, P.; Monesi, E.; Scardia, G.; Panagopoulou, E.; Harvati, K. Magnetostratigraphic and chronostratigraphic constraints on the Marathousa 1 Lower Palaeolithic site and the Middle Pleistocene deposits of the Megalopolis basin, Greece. *Quat. Int.* **2018**, *497*, 154–169. [CrossRef]
24. Koufos, G.D.; Kostopoulos, D.S.; Koliadimou, K.K. Un nouveau gisement de mammifères dans le Villafranchien de Macédoine occidentale (Grèce). *CR Acad. Sci. Paris* **1991**, *313*, 831–836.
25. Koufos, G.D. Late Pliocene carnivores from Western Macedonia (Greece). *Paläontol. Z.* **1993**, *67*, 357–376. [CrossRef]
26. Koufos, G.D.; Kostopoulos, D.S. A stenonoid horse (Equidae, Mammalia) from the Villafranchian of Western Macedonia (Greece). *Bull. Geol. Soc. Greece* **1993**, *28*, 131–143.
27. Koufos, G.D.; Kostopoulos, D.S. New Carnivore material from the Plio-Pleistocene of Macedonia (Greece) with the description of a new canid. *Münch. Geowiss. Abh. A Geol. Paläontol.* **1997**, *34*, 33–63.
28. Kostopoulos, D.S.; Koufos, G. The Plio-Pleistocene artiodactyls of Macedonia (Northern Greece) and their biostratigrphic significance; preliminary report. *CR Acad. Sci. Paris* **1994**, *318*, 1267–1272.
29. Kostopoulos, D.S.; Guy, F.; Kynigopoulou, Z.; Koufos, G.D.; Valentin, X.; Merceron, G. A 2Ma old baboon-like monkey from Northern Greece and new evidence to support the *Paradolichopithecus–Procynocephalus* synonymy (Primates: Cercopithecidae). *J. Hum. Evol.* **2018**, *121*, 178–192. [CrossRef]
30. Koufos, G.D.; Kostopoulos, D.S.; Merceron, G. The saber-toothed cat *Homotherium latidens* (Owen, 1864) from the lower Pleistocene locality Dafnero, Western Macedonia, Greece. *Geodiversitas* **2020**, *42*, 139–149. [CrossRef]
31. Rook, L.; Martínez-Navarro, B. Villafranchian: The long story of a Plio-Pleistocene European large mammal biochronologic unit. *Quat. Int.* **2010**, *219*, 134–144. [CrossRef]
32. Sinusía, C.; Pueyo, E.L.; Azanza, B.; Pocoví, A. Datación magnetoestratigráfica del yacimiento paleontológico de la Puebla de Valverde (Teruel). *Geotemas* **2006**, *6*, 329–342.
33. Pla-Pueyo, S.; Viseras, C.; Soria, J.M.; Tent-Manclús, J.E.; Arribas, A. A stratigraphic framework for the Pliocene-Pleistocene continental sediments of the Guadix Basin (Betic Cordillera, S. Spain). *Quat. Int.* **2011**, *243*, 16–32. [CrossRef]
34. Nomade, S.; Pastre, J.F.; Guillou, H.; Faure, H.M.; Guérin, C.; Delson, E.; Debard, E.; Voinchet, P.; Messager, E. 40Ar/39Ar constraints on some French landmark Late Pliocene to Early Pleistocene large mammalian paleofaunas: Paleoenvironmental and paleoecological implications. *Quat. Geochronol.* **2014**, *21*, 2–15. [CrossRef]
35. Zelilidis, A.; Piper, D.J.W.; Kontopoulos, N. Sedimentation and basin evolution of the Oligocene–Miocene Mesohellenic basin, Greece. *AAPG Bull.* **2002**, *86*, 161–182.
36. Ferrière, J.; Chanier, F.; Reynaud, J.-Y.; Pavlopoulos, A.; Ditbanjong, P.; Coutand, I. Evolution of the Mesohellenic Basin (Greece): A synthesis. In *The Geology of Greece-Part II*; Skourtsos, E., Ed.; The Virtual Explorer Pty Ltd.: Conder, Australia, 2013.
37. Kilias, A.D.; Vamvaka, A.; Falalakis, G.; Sfeikos, A.; Papadimitriou, E.; Gkarlaouni, C.; Karakostas, B. The Mesohellenic Trough and the Paleogene Thrace Basin on the Rhodope Massif, their Structural Evolution and Geotectonic Significance in the Hellenides. *J. Geol. Geosci.* **2015**, *4*, 198. [CrossRef]
38. Lowrie, W. Identification of ferrimagnetic minerals in rock by coercivity and unblocking temperature properties. *Geophys. Res. Lett.* **1990**, *17*, 159–162. [CrossRef]
39. Zijderveld, J.D.A. AC demagnetization rocks: Analyses of results. In *Methods in Paleomagnetism*; Collinson, D.W., Creer, K.M., Runcorn, S.K., Eds.; Elsevier Scientific: Amsterdam, The Netherlands, 1967; pp. 254–286.

40. Kirschvink, J.L. The least-square line and plane and analysis of palaeomagnetic data. *Geophys. J. R. Astron. Soc.* **1980**, *62*, 699–718. [CrossRef]
41. Fisher, R.A. Dispersion on a sphere. *Proc. R. Soc. Lond.* **1953**, *217*, 295–305. [CrossRef]
42. McFadden, P.L.; McElhinny, M.W. Classification of the reversal test in palaeomagnetism. *Geophys. J. Int.* **1990**, *103*, 725–729. [CrossRef]
43. Opdyke, N.D.; Channel, J.E.T. *Magnetic Stratigraphy*; Academic Press: San Diego, CA, USA, 1996.
44. Eltgen, H. *Feinstratigraphisch-Fazielle Untersuchungen an Pliozän-Sedimenten im Tertiärbecken Südlich Neapolis/Kozani, Nordgriechenland*; Institouton geōlogias kai ereunōn upedafous: Athens, Greece, 1986; pp. 107–115.
45. Fountoulis, I.; Markopoulou-Diakantoni, A.; Mpakopoulou, A.; Moraiti, E.; Mikrou, M.-P.; Saroglou, X. The presence of marine Pliocene sediments in the Messohelenic trough (Pramoritsa banks, Grevena, Greece). *Bull. Geol. Soc. Greece* **2001**, *24*, 603–612.
46. Guérin, C.; Tsoukala, E. The Tapiridae, Rhinocerotidae and Suidae (Mammalia) of the Early Villafranchian site of Milia (Grevena, Macedonia, Greece). *Geodiversitas* **2013**, *35*, 447–489. [CrossRef]
47. Lazaridis, G.; Tsoukala, E.; Maul, L.C.H. The earliest *Hystrix refossa*: A new Early Villafranchian record from Milia (Grevena, Macedonia, Greece). *Hystrix* **2019**, *30*, 12–18.
48. Koufos, G.D. The Villafranchian mammalian faunas and biochronology of Greece. *Boll. Soc. Paleontol. Ital.* **2001**, *40*, 217–223.
49. Sotnikova, M.; Rook, L. Dispersal of the Canini (Mammalia, Canidae: Caninae) across Eurasia during the Late Miocene to Early Pleistocene. *Quat. Int.* **2010**, *212*, 86–97. [CrossRef]
50. Madurell-Malapeira, J.; Ros-Montoya, S.; Espigares, M.P.; Alba, D.M.; Aurell-Garrido, J. Villafranchian large mammals from the Iberian Peninsula: Paleobiogeography, paleoecology and dispersal events. *J. Iber. Geol.* **2014**, *40*, 167–178. [CrossRef]
51. Bellucci, L.; Bona, F.; Corrado, P.; Magri, D.; Mazzini, I.; Parenti, F.; Scardia, G.; Sardella, R. Evidence of late Gelasian dispersal of African fauna at Coste San Giacomo (Anagni Basin, central Italy): Early Pleistocene environments and the background of early human occupation in Europe. *Quat. Sci. Rev.* **2014**, *96*, 72–85. [CrossRef]
52. Cohen, K.M.; Gibbard, P.L. Global chronostratigraphical correlation table for the last 2.7 million years, version 2019 QI-500. *Quat. Int.* **2019**, *500*, 20–31. [CrossRef]
53. Ferring, C.R. Rates of Fluvial Sedimentation: Implications for Archaeological Variability. *Geoarchaeology* **1986**, *1*, 259–274. [CrossRef]
54. Sen, S. Magnetostratigraphie et taux de sédimentation: Quelques données sur les dépôts fluviatiles, lacustres et marins du Néogène mediterranéen. *Bull. Société Géol. France* **1988**, *4*, 161–166. [CrossRef]
55. Sen, S.; de Bonis, L.; Dalfes, N.; Geraads, D.; Koufos, G.D. Les gisements de mammifères du Miocène supérieur de Kemiklitepe, Turquie: Stratigraphie et magnetostratigraphie. *Bull. Mus. Nat. Hist. Nat. Paris* **1994**, *16*, 5–17.
56. Arribas, A.; Garrido, G.; Viseras, C.; Soria, J.M.; Pla, S.; Solano, J.G.; Garcés, M.; Beamud, E.; Carrió, J.S. A Mammalian Lost World in Southwest Europe during the Late Pliocene. *PLoS ONE* **2009**, *4*, e7127. [CrossRef] [PubMed]
57. Martínez-Navarro, B. Early Pleistocene faunas of Eurasia and hominid dispersals. In *Out of Africa I: The First Hominin Colonization of Eurasia*; Vertebrate Paleobiology and Paleoanthropology Series; Fleagle, J.G., Shea, J.J., Grine, F.E., Baden, A.L., Leakey, R.E., Eds.; Springer Press: Amsterdam, The Netherlands, 2010; pp. 207–224.
58. Spassov, N. Zorillas (Carnivora, Mustelidae, Ictonychini) from the Villafranchian of Bulgaria with a description of a new species of Baranogale Kormos, 1934. *Geodiversitas* **2001**, *23*, 87–104.
59. Spassov, N. The Plio-Pleistocene vertebrate fauna in South-Eastern Europe and the megafaunal migratory waves from the east to Europe. *Revue Paleobiol.* **2003**, *22*, 197–229.
60. Popescu, S.-M.; Biltekin, D.; Winter, H.; Suc, J.-P.; Melinte-Dobrinescu, M.C.; Klotz, S.; Rabineau, M.; Combourieu-Nebout, N.; Clauzon, G.; Deaconu, F. Pliocene and Lower Pleistocene vegetation and climate changes at the European scale: Long pollen records and climatostratigraphy. *Quat. Int.* **2010**, *219*, 152–167. [CrossRef]
61. Rivals, F.; Athanassiou, A. Dietary adaptations in an ungulate community from the late Pliocene of Greece. *Palaeogeogr. Palaeoclimatol. Palaeoecol.* **2008**, *265*, 134–139. [CrossRef]

62. Berlioz, E.; Kostopoulos, D.S.; Blondel, C.; Merceron, G. Feeding ecology of *Eucladoceros ctenoides* as a proxy to track regional environmental variations in Europe during the early Pleistocene. *CR Palevol.* **2018**, *17*, 320–332. [CrossRef]
63. Hermier, R.; Merceron, G.; Kostopoulos, D.S. The emblematic Eurasian Villafranchian antelope *Gazellospira* (Mammalia: Bovidae): New insights from the Lower Pleistocene Dafnero fossil sites (Northern Greece). *Geobios* **2020**, in press. [CrossRef]
64. De Vos, J.; van der Made, J.; Athanassiou, A.; Lyras, G.; Sondaar, P.Y.; Dermitzakis, M.D. Preliminay note on the late Pliocene fauna from Vatera (Lesvos, Greece). *Ann. Geol. Pays Hell.* **2002**, *39*, 37–70.
65. Athanassiou, A. A Villafranchian *Hipparion*-bearing mammal fauna from Sésklo (E. Thessaly, Greece): Implications for the question of *Hipparion–Equus* sympatry in Europe. *Quaternary* **2018**, *1*, 12. [CrossRef]